Video Quality-Aware Traffic Steering System for Multi-Homed Mobile Terminal

Gi Seok Park
Senior Engineer
System Design Lab.
Network Business
Samsung Electronics
Suwon, Republic of Korea
giseok.park@samsung.com

Hyunmin Noh
Department of Computer Science and Engineering
POSTECH
Pohang, Republic of Korea
hmnoh@postech.ac.kr

Hwangjun Song
Department of Computer Science and Engineering
POSTECH
Pohang, Republic of Korea
hwangjun@postech.ac.kr

***Abstract*—This work presents a video quality-aware traffic steering system that provides stable video streaming services to users by steering part of the macrocell traffic into small cells. The proposed system achieves a good balance between fairness and social welfare in terms of the video quality by allocating the radio resource of the macro base station. The user data flow is split into two parts toward the macro base station and small cell AP, and the users simultaneously receive their data from both. In the proposed system, fountain code is employed to achieve dual connectivity enhancement by overcoming practical issues in the dual connectivity architecture. Furthermore, SDN technology is adopted not only to quickly react to time-varying network status but also to control network resources efficiently. The proposed resource allocation process is designed to require a low running time complexity. The proposed system is implemented using C/C++, Java, and a well-known ONOS open source. The experimental results verify that the proposed system can achieve much better performance than other traffic steering algorithms.**

Keywords—Dual connectivity, Software defined networking (SDN), Video streaming, Fountain code

I. INTRODUCTION

The widespread use of smart mobile devices along with the rapid rise in bandwidth-intensive multimedia services such as mobile video streaming, mobile gaming, and social networking has led to a tremendous increase in global mobile data traffic. According to the Cisco visual network index [1], the overall mobile video traffic is expected to increase at a compound annual growth rate of 54% from 2016 to 2021. This will account for more than 78% of the total mobile data traffic in 2021. Unfortunately, this rapid growth in mobile data traffic has caused a lack of radio resources in a network composed of only macrocells [2].

Deploying small cell access points (APs), e.g., femtocell, picocell, microcell, and 802.11 APs, within the coverage area of a macrocell has been considered as the most viable solution to accommodate a significant quantity of mobile data traffic in a cost-effective manner [3]. Global network operators such as AT&T, T-Mobile, Orange, and China Mobile have widely deployed carrier-grade access points in densely populated locations like malls, markets, and cafes to improve local capacity in traffic hotspots and relieve the burden on overloaded macro base station (MBS) [4].

For third generation partnership project (3GPP) long term evolution (LTE), the macro and small cell integration options have been extended in Release 12 with the introduction of dual connectivity (DC) [5], [6]. The main motivation behind the development of DC architecture is to enhance mobility robustness and increase end-to-end throughput by simultaneously serving users through MBS and small cell AP operating at different carriers. Much research effort has been devoted to the provision of mobility reliability and increasing the data rate in DC architecture. Hsieh et al. [5] designed a DC-based prevenient handover scheme to improve the handover robustness, where the radio resources of the target base station is obtained in advance by establishing dual connectivity to both the serving base station and the target base station. Singh et al. [6] proposed the anchor-booster framework maximizing proportional fairness by sharing the resource of macrocell, where each user's traffic is split across a macrocell and a small cell.

Previous studies have shown that the DC can improve end-to-end throughput and mobility performance, but challenging issues remain in the DC such as packet reordering and radio resource management [7], [8]. When the data flow is split into two parts toward MBS and a small cell AP, the head-of-line (HOL) blocking problem may be caused and consequently result in throughput degradation in transport and application layers [7]. This is not only due to the different channel status of macrocell and small cell APs but also to the non-ideal backhaul link between MBS and AP that makes a significant difference in packet arrival time. Besides, a resource allocation without considering network status and application characteristics may lead to an inefficient use of radio resources and consequently incur service quality degradation [8].

In this paper, we propose a video quality-aware traffic steering system for video streaming services. In the proposed system, fountain code [9] is adopted to overcome the HOL blocking problem and to split data flows on a flexible scale. Furthermore, software defined networking (SDN) technology [10] is employed not only to quickly respond to time-varying network status, but also to achieve efficient radio resource allocation through the intelligent controller with a global view of the network. The main technical contributions of this work are summarized as follows:

- We apply fountain code not only to overcome practical issues such as the HOL blocking and packet reordering inherent in the DC architecture but also to achieve better traffic aggregation by harmonizing the different network statuses of macro and small cells.
- We establish the resource allocation criteria, e.g., the video quality fairness and the highest social welfare, and analyze the impact of each allocation criterion on the video quality both theoretically and experimentally. Furthermore, we

tightly coordinate resource allocation criteria and achieve a good balance between them.

- We consider an SDN-enabled cellular network core for the implementation of the proposed system, where the controller gathers information related to the network status and application characteristics, and rapidly detects changes in network state. This information enables the proposed system to allocate the radio resources fairly and efficiently. The proposed system requires very low time complexity and thus can be run in real time.
- We implement the proposed system using NS-3 [11] to validate the system performance. For feasibility testing of the proposed system, a real testbed is constructed using ONOS open source platform and a Raspberry PI, where we offer an insight in implementing the practical system.

The rest of the paper is organized as follows. The details of the proposed video quality-aware traffic steering system are provided in Section II. The experimental results are presented in Section III, and concluding remarks are made in Section IV.

II. Proposed System Model

The ultimate goal of the proposed system is to provide stable video streaming services to users while achieving a good balance between the quality fairness and social welfare in the video quality. To achieve this goal, the proposed system allocates the radio resources of a macrocell to users, and appropriately splits user data flow into two parts toward the macrocell and a small cell. The overall architecture of the proposed system is shown in Fig. 1. The cellular network consists of MBSs, small cell APs operated on a different frequency from the MBS, users with dual network interfaces, and the EPC toward the remote media server. As the SDN is applied to the mobile network, the control functionalities of cellular network entities are separated from physical network equipment. Actually, SDN-enabled network core tends to be deployed in the recently emerging cellular networks [12]. In addition, the cloud EPC has been done on SDN-enabled mobile network not only to provide more intelligent, resilient, and scalable network but also to promptly introduce target and tailored network services [13]. Thus, we consider the cloud EPC as a platform for implementing the proposed system. The proposed system is composed of three main components: data collector, resource controller, and fountain encoding controller.

The overall system procedure is presented in Fig. 2. The

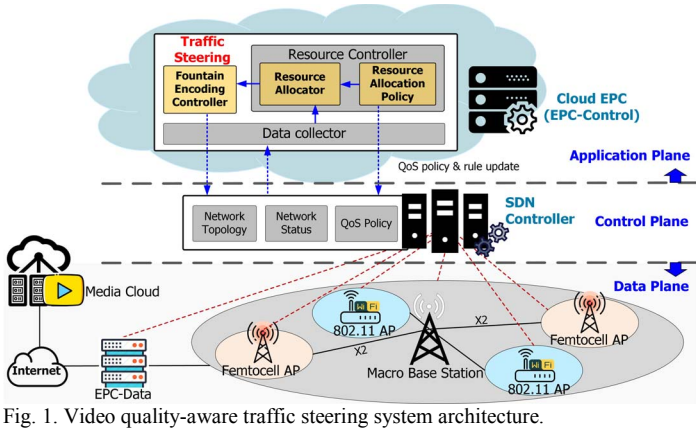

Fig. 1. Video quality-aware traffic steering system architecture.

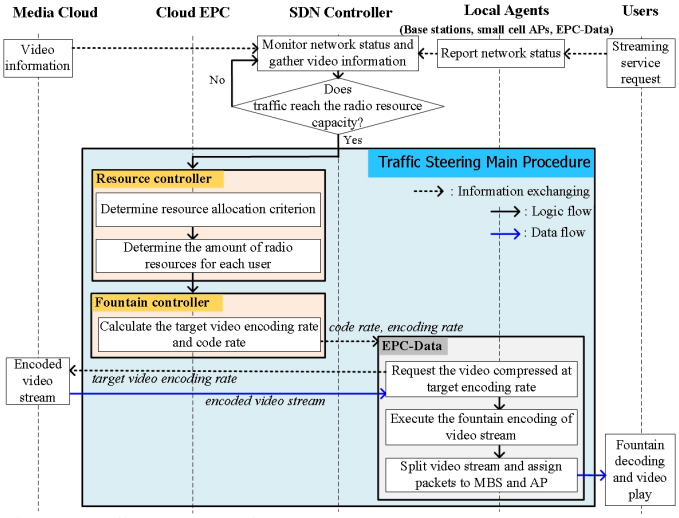

Fig. 2. Overall system procedure.

SDN controller periodically gathers network status information, e.g., bandwidth, delay, packet loss rate, from MBSs and small cell APs as well as video content characteristics, e.g., video encoding rate and rate-distortion model parameters, from the media server. When the network congestion is expected in radio access networks, the SDN controller immediately triggers the proposed system. At this time, the data collector module aggregates network status and video content information from the SDN controller. With this information, the resource allocation policy module calculates target video quality level that the MBS can support with small cell APs for users, and then establishes an allocation criterion for the allocation of the macrocell radio resources. Next, the resource allocator module determines the amount of radio resources for each user based on the allocation criterion. Considering both the resource allocation per user and the network status information, the fountain controller module determines the target video encoding rate and the amount of redundant encoding data, i.e., code rate, for fountain encoding, and then sends them to the EPC agent. When the video request arrives from users, the EPC agent requests the same video compressed at the target video encoding rate to the media server. When the requested video stream arrives, the EPC agent executes fountain encoding at pre-determined code rate, and splits the fountain encoded video stream into two parts directed toward the MBS and small cell AP. Finally, when the fountain encoded video stream arrives via the macro and small cell, the user executes the fountain decoding and plays the video stream.

A. Problem Description and Optimization

In this section, we describe the radio resource allocation problem in detail. First, some symbols are defined. $\boldsymbol{N}$ represents the set of users located in the coverage area of a macrocell. The instantaneous transmission rate for the i_{th} user from the small cell AP is denoted by R_i^{small}, which is periodically measured by the SDN controller. The macrocell radio resource allocated to the i_{th} user is represented by r_i^{macro}. To measure the objective video quality of the i_{th} user, we adopted the peak-signal-to-noise -ratio (PSNR):

$$f\left(r_i^{macro}\right)\Big|_{\text{with given } R_i^{small}} = 20\cdot\log\left(255\Big/\sqrt{D\left(R\left(r_i^{macro},R_i^{small}\right)\right)}\right), \quad (1)$$

where $D\left(R\left(r_i^{macro},R_i^{small}\right)\right)$ is an empirical group of pictures (GOP)-level rate-distortion model [14], that is,

$$D\left(R\left(r_i^{macro},R_i^{small}\right)\right)\approx\varepsilon_i\cdot R\left(r_i^{macro},R_i^{small}\right)^{\delta_i}, \quad (2)$$

where $\varepsilon_i\in\mathcal{R}^+$ and $\delta_i\in[-1,0]$ are rate-distortion model parameters and their value depends on the i_{th} user's video sequence. $R\left(r_i^{macro},R_i^{small}\right)$ means the video encoding rate for a GOP. It depends on the compressed video characteristics and the amount of redundant data from fountain encoding, and can be calculated as follows:

$$R\left(r_i^{macro},R_i^{small}\right)=\frac{\left(r_i^{macro}+R_i^{small}\right)\cdot c_i\left(r_i^{macro},R_i^{small}\right)}{\left(N^{frm}/R^{frm}\right)}, \quad (3)$$

where N^{frm} is the number of frames in a GOP and R^{frm} is the video frame rate, i.e., the number of frame per second. $c_i\left(r_i^{macro},R_i^{small}\right)$ represents the code-rate of fountain encoding. The code-rate is equal to the ratio of the amount of fountain encoded data to the amount of source data In [15], it is approximated as follows:

$$c_i\left(r_i^{macro},R_i^{small}\right)\approx\gamma_i\cdot\left(r_i^{macro}+R_i^{small}\right)^{\kappa_i}, \quad (4)$$

where $\gamma_i\in[0,1]$ and $\kappa_i\ (0<\kappa_i<<1)$ are model parameters dependent on the packet loss rate and fountain decoding success probability. Based on (1), we can measure the video quality improvement by providing additional macro resources to the user with R_i^{small} in the small cell:

$$u_i\left(r_i^{macro}\right)\Big|_{\substack{\text{with}\\ \text{given } R_i^{small}}} = f\left(r_i^{macro}\right)\Big|_{\substack{\text{with}\\ \text{given } R_i^{small}}} - f\left(0\right)\Big|_{\substack{\text{with}\\ \text{given } R_i^{small}}} = 20\cdot\log\left(R_i^{small}\Big/r_i^{macro}+R_i^{small}\right)^{\delta_i\cdot(1+\kappa_i)/2}. \quad (5)$$

1) Problem formulation

We can formulate the **radio resource allocation problem**.

Given: R_i^{small} and β_i for $\forall i\in\boldsymbol{N}$.

Determine: r_i^{macro} for $\forall i\in\boldsymbol{N}$ so as to

$$\text{maximize}\ \sum_{i=1}^{|\mathcal{N}|}\beta_i\cdot u_i\left(r_i^{macro}\right)\Big|_{\text{with given } R_i^{small}} \quad (6)$$

$$\text{subject to}\ \sum_{i=1}^{|\mathcal{N}|}r_i^{macro}\le R_{\max}^{macro} \quad (7)$$

$$\text{and}\ r_i^{macro}\ge 0\ \text{ for }\forall i\in\boldsymbol{N}, \quad (8)$$

where $R_{\max}^{macro}$ is the amount of available bandwidth for video streaming services in a macrocell. The individual weighting factor for each user's video quality is β_i, and the total sum of weighting factors is one. In fact, the user with a higher weighting factor gets more radio resources from the macrocell, and vice versa. In this context, our resource allocation problem can be represented by the Nash bargaining model [16], where β_i and $R_{\max}^{macro}$ are considered as the bargaining power and the competitive resource among users, respectively. Now, we redefine the above resource allocation problem as **bargaining problem**.

Given: R_i^{small} and β_i for $\forall i\in\boldsymbol{N}$.

Determine: r_i^{macro} for $\forall i\in\boldsymbol{N}$ so as to

$$\text{maximize}\ \prod_{i=1}^{|\mathcal{N}|}\left(\hat{u}_i\left(r_i^{macro}\right)\Big|_{\text{with given } R_i^{small}}\right)^{\beta_i} \quad (9)$$

$$\text{subject to}\ \sum_{i=1}^{|\mathcal{N}|}r_i^{macro}\le R_{\max}^{macro} \quad (7)$$

$$\text{and}\ r_i^{macro}\ge 0\ \text{ for }\forall i\in\boldsymbol{N}, \quad (8)$$

where $\hat{u}_i\left(r_i^{macro}\right)\Big|_{\text{with given } R_i^{small}}$ represents $\dfrac{R_i^{small}}{r_i^{macro}+R_i^{small}}^{\delta_i\cdot(1+\kappa_i)/2}$ in (5) and is referred to as the i_{th} user utility. In the bargaining model, (9) is interpreted as the Nash product [16]. To show that the bargaining problem is equivalent to the resource allocation problem, we take the logarithm and multiply a constant in (9):

$$20\cdot\log\prod_{i=1}^{|\mathcal{N}|}\left(\hat{u}_i\left(r_i^{macro}\right)\Big|_{\text{with given } R_i^{small}}\right)^{\beta_i} = \sum_{i=1}^{|\mathcal{N}|}\beta_i\cdot u_i\left(r_i^{macro}\right)\Big|_{\text{with given } R_i^{small}}. \quad (10)$$

As a result, (6) is derived from (9) by the logarithmic property. That is, there is no solution gap and only a difference in scale between (6) and (9).

2) Optimal control variable determining process

We describe how to determine the optimal solution for the bargaining problem. Note that Nash product in (9) is a monotonically non-decreasing concave for $r_i^{macro}\ge 0$ because the first derivative is positive, and the second derivative is negative. It is well known in the optimization theory [17] that the optimal solution is obtained by the water-filling method when the objective function is the non-decreasing concave and the constraint set is convex. Based on the water-filling method, we design the macro resource allocation algorithm. Its basic idea is to divide the macro resource into several small resource units, and assign them to the users in a greedy manner.

B. Bargaining Power Determining Process

As shown in section II.A.1, it is assumed that the bargaining power values are given. In this section, we analyze the bargaining power effect on the user utility, and describe how to determine bargaining power according to various criteria. First, we define the Nash bargaining set as follow:

$$\boldsymbol{B}=\left\{\hat{\boldsymbol{u}}=\left(\hat{u}_1,\cdots,\hat{u}_{|\mathcal{N}|}\right)\Big|\sum_{i=1}^{|\mathcal{N}|}R_i^{small}\cdot\left(\hat{u}_i^{\frac{-2}{\delta_i\cdot(1+\kappa_i)}}-1\right)=R_{\max}^{macro},\ \hat{u}_i\ge 0\ \text{for}\ \forall i\in\boldsymbol{N}\right\}, \quad (11)$$

where $\hat{u}_i\left(r_i^{macro}\right)\Big|_{\text{with given } R_i^{small}}$ is simply denoted by $\hat{u}_i$. The bargaining set represents all cases of utility that users can achieve when $R_{\max}^{macro}$ is fully allocated. In [16], it is shown that

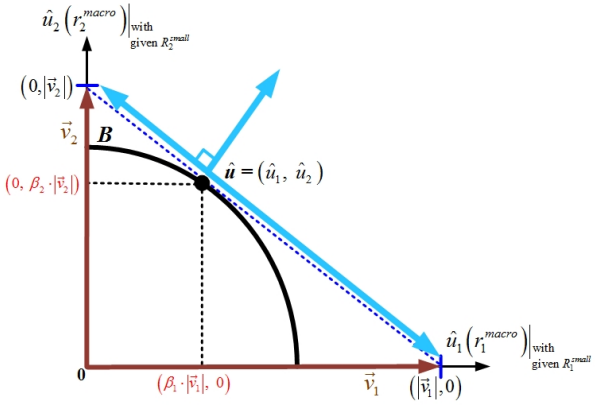

Fig. 3. Geometric interpretation of the bargaining set when $|\boldsymbol{N}|=2$.

the solution candidates satisfying the Pareto optimality are located in the bargaining set, and the bargaining power determines a unique solution point in the bargaining set. Fig. 3 shows the relation between the bargaining power and $\hat{\boldsymbol{u}}$ from a geometrical perspective, where $|\vec{v}_i|$ is the intersection with the tangent line at $\hat{\boldsymbol{u}}$ on the i-axis, that is, $\vec{v}_i=\left(0,\cdots,\dfrac{\hat{u}_i}{\beta_i},\cdots,0\right)$. As shown in the figure, the i_{th} bargaining power is equal to the ratio of $|\vec{v}_i|$ to $\hat{u}_i$, that is, $\beta_i=\hat{u}_i/|\vec{v}_i|$ for $\forall i\in\boldsymbol{N}$.

The resource allocation criteria can be defined in various ways. In this work, we consider the most popular two criteria for resource allocation: video quality fairness and highest social welfare. We derive bargaining power for each criterion.

1) Bargaining power for video quality fairness

First, we derive the bargaining power ($\beta_1^{vq},\cdots,\beta_{|\boldsymbol{N}|}^{vq}$) achieving similarity among users in the video qualities, i.e.,

$$f\left(r_1^{macro}\right)\big|_{\text{with given } R_1^{small}}=\cdots=f\left(r_{|\boldsymbol{N}|}^{macro}\right)\big|_{\text{with given } R_{|\boldsymbol{N}|}^{small}}. \quad (12)$$

To find the point satisfying (12) on the bargaining set, we calculate the target video quality level (Q^{target}) that users can equally achieve. Algorithm 1 presents a fast algorithm for acquiring Q^{target} with low complexity. It shows ε trade-off between time complexity and accuracy and requires a computational complexity of $O\left(R_{\max}^{macro}/\varepsilon\right)$.

Based on (5), we can now calculate the unique point $\hat{\boldsymbol{u}}_{vq}=\left(\hat{u}_1^{vq},\cdots,\hat{u}_i^{vq},\cdots,\hat{u}_{|\boldsymbol{N}|}^{vq}\right)$ satisfying target video quality in the bargaining set as follows:

$$\hat{u}_i^{vq}\left(r_i^{macro}\right)\big|_{\text{with given } R_i^{small}}=10^{\frac{\left(Q^{target}-PSNR(0)\big|_{\text{with given } R_i^{small}}\right)}{20}},\ \forall i\in\boldsymbol{N}. \quad (13)$$

Since the gradient vector at $\hat{\boldsymbol{u}}_{vq}$ in the bargaining set is perpendicular to the supporting plane at $\hat{\boldsymbol{u}}_{vq}$, we obtain

$$\nabla\boldsymbol{B}\big|_{\hat{\boldsymbol{u}}_{vq}}\bullet\left(\vec{v}_i-\hat{\boldsymbol{u}}_{vq}\right)=0,\ \forall i\in\boldsymbol{N}, \quad (14)$$

Algorithm 1. Target Video Quality Decision

Input $R_{\max}^{macro}$, R_1^{small},..., $R_{|\boldsymbol{N}|}^{small}$, ε

Output Q^{target}

Initialize $Q^{\min}\leftarrow 0$, $Q^{\max}\leftarrow\max_{\forall i\in\boldsymbol{N}}\left\{PSNR\left(R_{\max}^{macro}\right)\big|_{\text{with given } R_i^{small}}\right\}$
Do
  $R^{new}\leftarrow 0$, $Q^{new}\leftarrow\left(Q^{\min}+Q^{\max}\right)/2$
  For $\forall i\in\boldsymbol{N}$
    $Q_i^{gap}\leftarrow\max\left\{\left(Q^{new}-PSNR(0)\big|_{\text{with given } R_i^{small}}\right),0\right\}$
    $R^{new}\leftarrow R^{new}+u_i^{-1}\left(Q_i^{gap}\right)\big|_{\text{with given } R_i^{small}}$
  End For
  If $R^{new}<R_{\max}^{macro}$ **then**
    $Q^{\min}\leftarrow Q^{new}$
  Else
    $Q^{\max}\leftarrow Q^{new}$
  End If
While $\left|R_{\max}^{macro}-R^{new}\right|/R_{\max}^{macro}>\varepsilon$
$Q^{target}\leftarrow Q^{new}$

where $\nabla\boldsymbol{B}\big|_{\hat{\boldsymbol{u}}_{vq}}$ represents $\left(\dfrac{\partial\boldsymbol{B}}{\partial\hat{u}_i}\Big|_{\hat{\boldsymbol{u}}_{vq}},\cdots,\dfrac{\partial\boldsymbol{B}}{\partial\hat{u}_i}\Big|_{\hat{\boldsymbol{u}}_{vq}},\cdots,\dfrac{\partial\boldsymbol{B}}{\partial\hat{u}_{|\boldsymbol{N}|}}\Big|_{\hat{\boldsymbol{u}}_{vq}}\right)^T$. This orthogonal property is shown in Fig. 3. Based on (14), the bargaining power for video quality fairness is calculated as follows:

$$\beta_i^{vq}=\left(\frac{\partial\boldsymbol{B}}{\partial\hat{u}_i}\Big|_{\hat{\boldsymbol{u}}_{vq}}\cdot\hat{u}_i^{vq}\right)\Bigg/\left(\sum_{k=1}^{|\boldsymbol{N}|}\frac{\partial\boldsymbol{B}}{\partial\hat{u}_k}\Big|_{\hat{\boldsymbol{u}}_{vq}}\cdot\hat{u}_k^{vq}\right), \quad (15)$$

2) Bargaining power for highest social welfare

Next, we derive the bargaining power ($\beta_1^{sw},\cdots,\beta_{|\boldsymbol{N}|}^{sw}$) maximizing the sum of the video quality, that is, $\sum_{i=1}^{|\boldsymbol{N}|}f\left(r_i^{macro}\right)\big|_{\text{with given } R_i^{small}}$. From (5), we have

$$f\left(r_i^{macro}\right)\big|_{\text{with given } R_i^{small}}=u_i\left(r_i^{macro}\right)\big|_{\text{with given } R_i^{small}}+f(0)\big|_{\text{with given } R_i^{small}}. \quad (16)$$

Since $f(0)\big|_{\text{with given } R_i^{small}}$ is a constant, the highest social welfare is achieved when $\sum_{i=1}^{|\boldsymbol{N}|}u_i\left(r_i^{macro}\right)\big|_{\text{with given } R_i^{small}}$ is maximized. It is exactly the same as maximizing (6) without considering the weighing factor. Since the multiplication of the objective function by a constant does not affect the solution, we obtain the bargaining power for highest social welfare as follows:

$$\beta_i^{sw}=\frac{1}{|\boldsymbol{N}|}\ \text{for}\ \forall i\in\boldsymbol{N}. \quad (17)$$

Now, we pursue an effective tradeoff between the video quality fairness and the highest social welfare by

$$\beta_i=\omega\cdot\beta_i^{vq}+(1-\omega)\cdot\beta_i^{sw}\ \text{for}\ \forall i\in\boldsymbol{N}, \quad (18)$$

where $\omega\in[0,1]$ is a bargaining power coordinator. As ω becomes close to 1, the video quality fairness among the users is improved but the social welfare decreases, and vice versa.

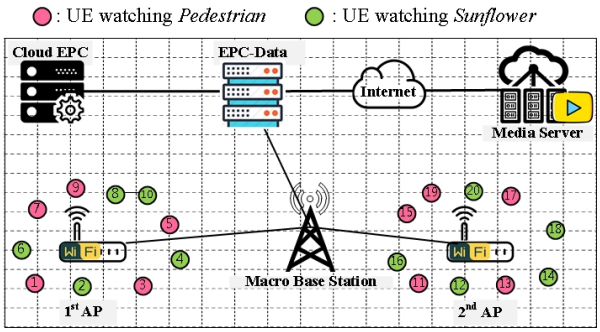

Fig. 4. Network topology for simulation.

III. Performance Evaluation

We implement the proposed system using NS-3 and demonstrate its performance. The network topology consists of the remote media server, controller, macro base station, and two 802.11 APs. Considering the mobile network environment presented in [18], the controller is connected to the EPC and communicates with the MBS and APs. Fig. 4 shows the network topology, where 10 users are connected to the 1st AP and 2nd AP, respectively. The users are randomly located within 50 m of the AP and the user mobility is arbitrarily set between 1 and 3 m/s. The Friis propagation loss model and a trace-driven fading loss model specified by 3GPP are employed for the macrocell network, and the yet another network simulator model is employed for small cell network. During the simulation, $R_{\max}^{macro}$ is fixed to 10 Mbps. The simulation is performed over 180 s.

- **Fountain code:** LT code is employed during the simulation. The symbol size and packet payload size are set to 32 bytes and 1024 bytes, respectively. Thus, a single packet includes 32 encoding symbols. The fountain decoding success probability is set to 0.99 and the code rate is adjusted in the range of 0.3 to 0.95 according to the wireless channel status.

TABLE I
PERFORMANCE SUMMARY ACCORDING TO THE BARGAINING POWER COORDINATOR

Coordinator value	0	0.25	0.5	0.75	1
Sum of PSNR	730.137	729.012	728.553	726.626	724.386
Sta. dev. of PSNR	2.2103	1.9907	1.7879	1.6252	1.5810

- **Test video:** During the simulation, we use two full high-definition (HD)-sized (1920×1080) video sequences; Pedestrian and Sunflower. The video stream is encoded using the H.264/MPEG-4 AVC codec at a rate of 25 frames per second, and a GOP consists of 25 frames (IPPP…PPP). The video playback time is 180 s, and each segment playback time is fixed to 1 s.

A. Performance Verification of the Proposed System

In this section, we demonstrate the performance of the proposed traffic steering system. First, we investigate the impact of bargaining power on the macro radio resource allocated to users. Fig. 5(a) shows the transmission rates for each user in small cell APs. The users receive the data at different transmission rates from the APs according their mobility. Fig. 5(b) shows the distribution of bargaining power assigned to each user for video quality fairness. Note that a relatively high bargaining power is assigned to users receiving data at a low transmission rate from the APs or watching the pedestrian video. The pedestrian video sequence has higher motion complexity than the sunflower video sequence. To reduce the video quality deviation among the users, more resources are allocated to the users who are assigned higher bargaining power. Thus, all of the users experience a similar video quality regardless of their video sequence and network status. This is clearly apparent in Figs. 5(c) and 5(d). On the other hand, Fig. 6(a) shows the distribution of the bargaining power for the highest social welfare. When the highest social welfare is considered, the bargaining power is uniformly

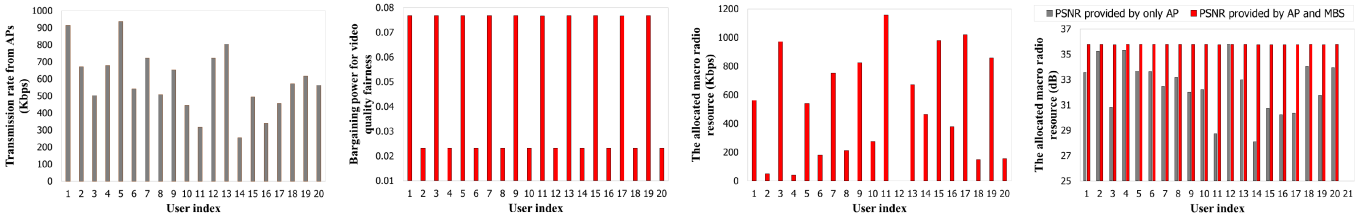

(a) (b) (c) (d)

Fig. 5. The impact of bargaining power for video quality fairness on the macro radio resource allocated to users: (a) transmission rate from APs, (b) the bargaining power, (c) the allocated macro radio resource, and (d) the video quality.

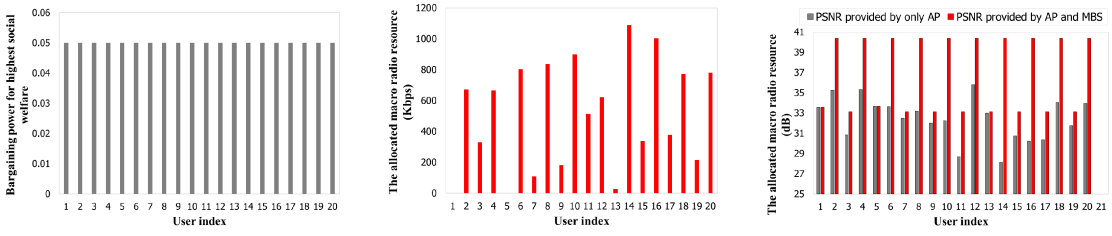

(a) (b) (c)

Fig. 6. The impact of bargaining power for highest social welfare: (a) the bargaining power, (b) the allocated macro radio resource, and (c) the video quality.

distributed to all users ($1/|\boldsymbol{N}|$). As shown in Fig. 6(b), to maximize the social welfare, the greatest allocation of radio resource is given to the users watching the sunflower video sequence with a low transmission rate from the APs. This is because their video quality is greatly improved although the same resources are allocated. Consequently, the users experience different video quality. In general, the users watching the sunflower video sequence have higher PSNR than the users watching the pedestrian sequence. This is shown in Fig. 6(c).

Now, we consider the impact of the bargaining power coordinator on the radio resource allocated to users. Table I shows the change of video quality according to the value of ω. The tendency between the quality fairness and social welfare according to ω is clearly apparent. As the value of ω approaches 1, the video quality deviation among the users is reduced but the overall video quality is degraded, and vice versa. That is, there exists a trade-off between the quality fairness and the social welfare in the range of ω (i.e., $\omega \in [0,1]$).

Next, we compare our system with the following three resource allocation algorithms:

- **AP-only**: Baseline algorithm for comparison. The users only receive their video data via small cell AP.
- **Static partial–flow (SP) splitting** [19]: The resource of MBS is equally allocated to users associated with the macrocell (i.e., $R_{\max}^{macro}/|\boldsymbol{N}|$). The users concurrently receive their data via MBS and small cell AP.
- **Proportional farness (PF) splitting** [6]: The resource of MBS is allocated to provide proportional fairness among users associated with the macrocell. Based on the amount of allocated resources, the user data is split into two parts toward the MBS and AP.

The comparison results are presented in Fig. 7. In the AP-only, users are only supported by small cell APs without the help of MBS. Thus, their video quality has a strong dependency on the channel state in the small cell. As shown in Fig. 7, the users experience relatively low video quality because of the small cell dynamic channel state and low data rate. In the SP splitting, the users experience higher video quality compared with the AP-only because they are provided with additional resource from the macrocell. However, the SP splitting cannot improve the overall video quality since the network status and the video characteristics are not considered. Besides, there is a significant difference in the video quality that users experience, as shown in Fig. 7(b). In the PF splitting, the overall social welfare is improved and the deviation of video quality among the users is reduced because the proportional fairness of the data rate is considered. However, the data rate fairness does not guarantee the highest social welfare and video quality fairness among the users. That is because each video has different video characteristics such as bitrate and resolution. The proposed system with ω set to 1 considers the fairness of the video quality instead of data rate. It is observed that the box plots in Fig. 7(d) are more uniformly distributed than the box plots in Fig. 7(c). This means that the quality deviation of the proposed system with ω set to 1 is lower than that of the PF splitting. The simulation results for the comparison are summarized in Table II. The performance of the PF splitting is similar to that of the proposed system with ω set to 0.5.

B. Feasibility Test on a Real Testbed

A real testbed is constructed using the media server, the controller, the EPC-Data, and a Raspberry PI-3-based MBS and AP, as shown in Fig. 8. We employ ONOS Magpie and implement the traffic steering system at the controller. As shown in Fig. 8, the MBS and AP are constructed by a two-layer Raspberry PI stack in which the OpenvSwitch (OVS) open source platform is installed at the bottom of the stack and an 802.11 AP is installed at the top of the stack using the hostapd software. Since OVS is a software-based switch that supports the OpenFlow protocol, the MBS and AP can communicate with the controller and forward the IP packets based on the flow table. To distinguish data flows toward MBS and AP, the flow table of OVS is configured. For the dual connectivity of users, two 802.11 interfaces are configured on the user and each is connected to the MBS and the AP. Video streaming applications for the media server and users are developed using Java and C/C++. Real-time transport protocol (RTP) video stream packets are produced at the media server

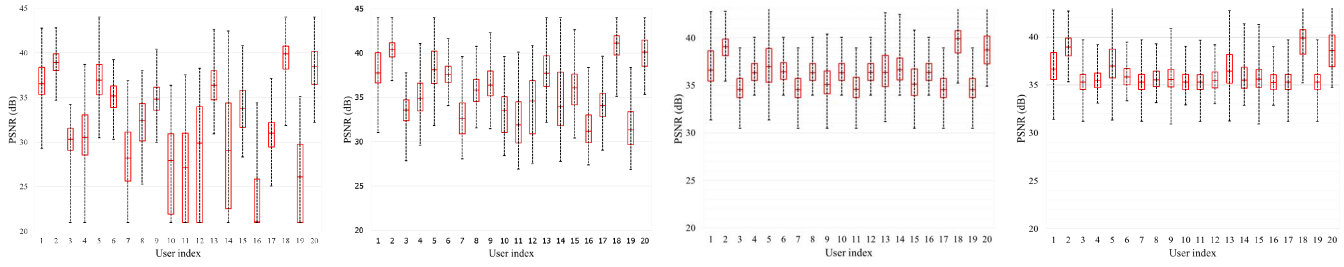

(a) (b) (c) (d)

Fig. 7. PSNR comparison with resource allocation algorithms: (a) AP only, (b) SP splitting, (c) PF splitting, and (d) proposed system with ω set to 1.

TABLE II
SUMMARY OF COMPARISON RESULTS

Algorithms	AP only	SP splitting	PF splitting	Proposed system		
				$\omega=0$	$\omega=0.5$	$\omega=1$
Social welfare	645.0431	715.1216	728.5528	730.137	728.5525	724.386
Sta. dev. of PSNR	3.3933	3.4776	1.8470	2.2103	1.7879	1.5810

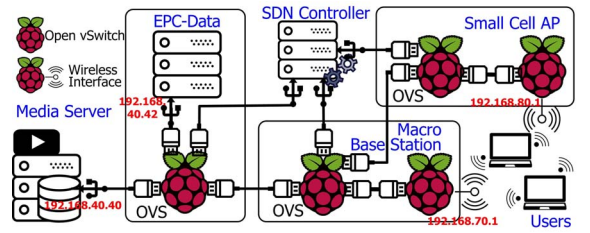

(a)

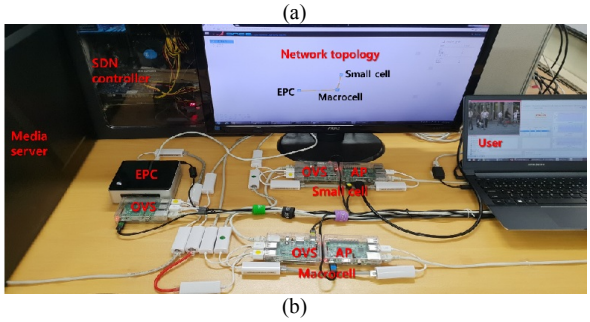

(b)

Fig. 8. Construction of a testbed: (a) layout drawing and (b) actual image.

and transmitted to the EPC-Data. The fountain encoded video stream is generated on the EPC-Data and is split into two parts toward the MBS and small cell AP. The fountain decoding is executed on the user side.

We verify the performance of the proposed system in a dynamic and real wireless network environment. During the experiment, the NetEM software is employed to emulate the macrocell and small cell networks. At the 802.11 interface installed at the top of a Raspberry PI stack, the network state are adjusted as shown in Table III. The test video sequence with 4CIF-size are generated by the crew video sequence, which are encoded at 25 fps (frames per second). The encoding structure is IPPP…PPP, i.e., 1 GOP includes 25 frames.

Figs. 9 shows the amount of allocated resources and the corresponding video quality in the quality fairness and highest social welfare, respectively. Similar to the simulation results in Section III.A, when ω is set to 1, the bargaining power is assigned so as to minimize the difference in video quality between users. Thus, a user with a low transmission rate from the AP gets more resources from the MBS. As a result, there is no difference in the video quality that two users experience. This can be observed in Fig. 9(a) and (b). Conversely, when ω is set to 0, the same bargaining power of 0.5 is assigned to maximize the sum of video quality. Figs. 9(c) and (d) show the amount of the resource allocated to each user and the corresponding video quality, respectively. It is apparent that the overall video quality is improved, while the quality deviation between users significantly increases.

To provide a subjective video quality comparison, the captured frames at 24 s with different ω are presented in Figs. 10 and 11. As can be seen in the figures, when ω is set to 1, a similar video quality of users is achieved, with figures such as the 1st user getting 33.05 dB and the 2nd user getting 33.06 dB. The sum of PSNR is 66.11 dB. Conversely, when ω is set to 0, the sum of PSNR values is maximized while increasing deviation, with figures such as the 1st user getting 32.26 dB and the 2nd user getting 35.50 dB. The sum of PSNR is 67.76 dB. The tendency between quality fairness and social welfare according to ω is well maintained in the real environment.

TABLE III
NETWORK CONDITION SCENARIOS

Network	Time (s)	Bandwidth (Kbps)	Delay (ms)	Packet loss rate (%)
Total radio resource of macro base station $R_{\max}^{MBS}$	0~30 30~60 60~	500	20	0.1~0.2
Small Cell AP (1st user)	0~30 30~60 60~	100 200 100	10	0.1~0.2
Small Cell AP (2nd user)	0~30 30~60 60~	200 100 200	10	0.1~0.2

IV. Conclusions

In this work, we have studied a video quality-aware traffic steering system for multi-homed mobile terminals, where the user concurrently receives the video data through a small cell AP and a macro base station. We adopted fountain codes, a type of forwarding error correction code, to overcome the goodput degradation caused by the packet reordering and head-of-line blocking inherent in multi-path video streaming. In our proposed system, the radio resource of a macrocell is fairly and efficiently allocated to the users considering the network status and the video characteristics. We established resource allocation criteria, i.e., video quality fairness and the highest social welfare, and presented a framework that achieves tight coordination between them. The proposed system was designed to require low time complexity and thus can operate in real-time. The simulation results demonstrated that the proposed system improves the video quality of more users than baseline algorithms. For feasibility testing, we built a real testbed using the well-known ONOS open source platform and presented the applicability of the proposed system in a mobile network. In future work, we intend to adaptively change the bargaining power coordinator according to the network status.

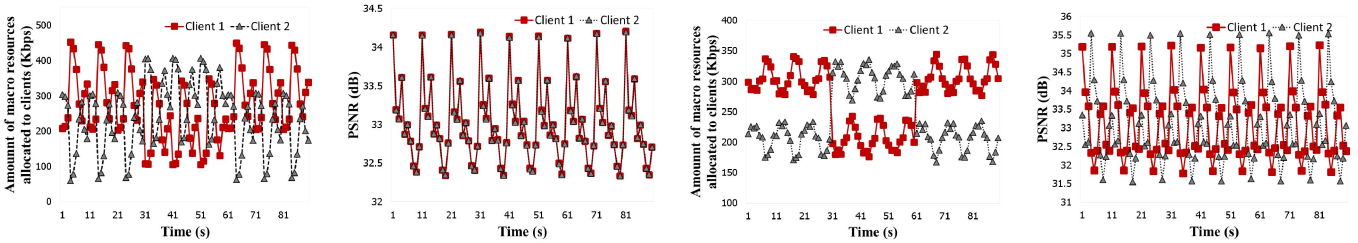

(a) (b) (c) (d)

Fig. 9. Performance evaluation of the proposed system: (a) the amount of allocated macro resources when ω=1, (b) PSNR when ω=1, (c) the amount of allocated macro resources when ω=0, and (b) PSNR when ω=0.

(a) (b)

Fig. 10. Subjective video quality comparison at 24 s when ω=1: (a) 1st user: 33.05 dB and (b): 2nd user: 33.06 dB.

(a) (b)

Fig. 11. Subjective video quality comparison at 24 s when ω=0: (a) 1st user: 32.26 dB and (b) 2nd user: 35.50 dB.

ACKNOWLEDGMENT

This work was partly supported by Institute for Information & communications Technology Promotion(IITP) grant funded by the Korea government(MSIT) (No. 2015-0-00567, Development of Access Technology Agnostic Next-Generation Networking Technology for Wired-Wireless Converged Networks) and National Research Foundation of Korea (NRF) grant funded by the Korea government(MSIP) (No. 2016R1A2B4007812).

REFERENCES

[1] Cisco White Paper, "Cisco Visual Networking Index–Global mobile data traffic forecast, update, 2016–2021," 2017.

[2] G. Bartoli, R. Fantacci, K. B. Letaief, D. Marabissi, N. Privitera, M. Pucci, and J. Zhang, "Beamforming for small cell deployment in LTE-Advanced and beyond," IEEE Wireless Communications, vol. 21, no. 2, Apr. 2014.

[3] H. Zhang, X. Chu, W. Guo, and S. Wang "Coexistence of Wi-Fi and heterogeneous small cell networks sharing unlicensed spectrum," IEEE Communications Magazine, vol. 53, no. 3, Mar. 2015.

[4] Tefficient industry analysis, "Using public Wi-Fi as customer magnet," 2016.

[5] P. Hsieh, W. Lin, K. Lin, and H. Wei, "Dual-connectivity prevenient handover scheme in control/user-plane split networks," IEEE Transactions on Vehicular Technology, vol. 67, no. 4, Apr. 2018.

[6] S. Singh, M. Geraseminko, S. Yeh, N. Himayat, and S. Talwar, "Proportional fair traffic splitting and aggregation in heterogeneous wireless networks," IEEE Commun. Letters, vol. 20, no. 5, May 2016.

[7] X. Wang, S. Mao, and M. Gong, "A survey of LTE Wi-Fi coexistence in unlicensed bands," ACM GetMobile: Mobile Computing and Communication, vol. 20, no. 3, 17–23, Jul. 2016.

[8] D. López-Pérez, D. Laselva, E. Wallmeier, P. Purovesi, P. Lundén, E. Virtej, P. Lechowicz, E. Malkamaki, and M. Ding, "Long term evolution-wireless local area network aggregation flow Control," IEEE Access, vol. 4, 9860–9869, 2016.

[9] D. MacKay, "Fountain codes," IEEE Commun., vol. 152, no. 6, 1062–1068, 2005.

[10] Open Networking Foundation, "Software-defined networking: the new norm for networks," White Paper, Apr. 2012.

[11] The network simulator 3 (NS-3), Available: http://www.nsnam.org

[12] J. He and W. Song, "Optimizing video request routing in mobile networks with built-in content caching," IEEE Tr. on Mobile Computing, vol. 15, no. 7, Jul. 2016.

[13] B. Han, V. Gopalakrishnan, L. Ji, and S. Lee, "Network function virtualization: challenges and opportunities for innovations," IEEE Communications Magazine, vol. 53, no. 2, 90–97, Feb. 2015.

[14] D. Jurca and P. Frossard, "Media flow rate allocation in multipath networks," IEEE Tr. on Multimedia, vol. 9, no. 6, 1227–1240, Oct. 2007.

[15] D. Ho, G. Park, and H. Song, "Game-theoretic scalable offloading for video streaming services over LTE and WiFi networks," IEEE Trans. on Mobile Computing, 2018.

[16] K. Binmore, "Fun and games: a text on game theory," Lexington, MA: Health, 1992.

[17] S. Boyd and L. Vandenberghe, "Convex optimization," Cambridge, U.K.: Cambridge Univ. Press, 2004.

[18] V. G. Vassilakis, I. D. Moscholios, B A. Alzahrani, and M. D. Logothetis, "Toward information-centric software-defined cellular networks," in Proc. IEEE ConTEL, 2017.

[19] S. C. Jha, K. Sivanesan, R. Vannithamby and A. T. Koc "Dual connectivity in LTE small cell networks," in Proc. Globecom Workshop–Heterogeneous and Small Cell Networks, 2014.